

Supplementary Information:

**High-capacity and ultrastable lithium storage in SnSe<sub>2</sub>-SnO<sub>2</sub>@NC microbelts enabled by heterostructure**

Haibin Sun,<sup>a,1,\*</sup> Wenjie Wang,<sup>a,1</sup> Lianduan Zeng,<sup>b,1</sup> Congcong Liu,<sup>a</sup> Shuangshuang Liang,<sup>a</sup> Wenhe Xie,<sup>a</sup> Shasha Gao,<sup>a</sup> Shenghong Liu,<sup>a,\*\*</sup> Xiao Wang<sup>b,\*\*\*</sup>

<sup>a</sup> *Key Laboratory of Microelectronics and Energy of Henan Province, School of Physics and Electronic Engineering, Xinyang Normal University, Xinyang 464000, China*

<sup>b</sup> *Shenzhen Key Laboratory of Nanobiomechanics, Shenzhen Institute of Advanced Technology, Chinese Academy of Sciences, Shenzhen 518055, China*

\*Corresponding authors :

*E-mail addresses:* [sunhaibin@xynu.edu.cn](mailto:sunhaibin@xynu.edu.cn) (H. Sun), [liush@xynu.edu.cn](mailto:liush@xynu.edu.cn) (S. Liu) & [xiao.wang@siat.ac.cn](mailto:xiao.wang@siat.ac.cn) (X. Wang)

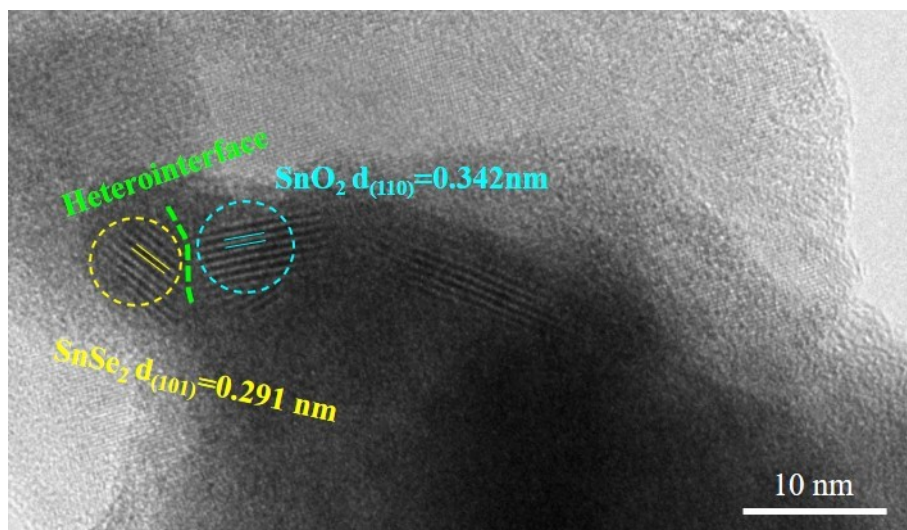


**Fig. S1.** High-resolution TEM image of SnSe<sub>2</sub>-SnO<sub>2</sub>@NC microbelts.

## Analysis of carbon contents in all samples:

As shown in **Fig. 2c**, the TGA curve of SnSe<sub>2</sub>-SnO<sub>2</sub>@NC is mainly divided into two parts in the temperature range of 25 to 800 °C:

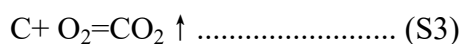
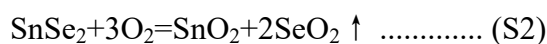
1. Evaporation of water below 200 °C ( $m_1$  (H<sub>2</sub>O)).

$$m_1(\text{wt}\%) \text{ (record from the y-axis, 93.15 wt}\%) = m(\text{SnSe}_2\text{-SnO}_2\text{@NC}) - m(\text{H}_2\text{O})\text{..... (S1)}$$

2. The oxidation of SnSe<sub>2</sub>-SnO<sub>2</sub>@NC to SnO<sub>2</sub> in the temperature range of 250 –800 °C

and the gasification of carbon ( $m_c$ ), also occurring in this temperature region.

Accordingly, the chemical reaction should be depicted as Equations (S2 or S3):



$$m_2(\text{wt}\%) \text{ (record from the y-axis, 32.15 wt}\%) = m(\text{SnO}_2) \\ = M(\text{SnO}_2) * n(\text{SnO}_2)\text{.....(S4)}$$

When Only SnSe<sub>2</sub> in the material, the SnSe<sub>2</sub> content of SnSe<sub>2</sub>-SnO<sub>2</sub>@NC is estimated by

$$m(\text{SnSe}_2) = (n(\text{SnO}_2) \times 1 \times M(\text{Sn})) / m_1(\text{wt}\%) \times 100 \text{ wt}\% = (m_2(\text{wt}\%) / M(\text{SnO}_2) \times 1 \times \\ M(\text{SnSe}_2)) / m_1(\text{wt}\%) \times 100 \text{ wt}\% = (m_2(\text{wt}\%) / 150.7 \times 1 \times (276.62) / m_1(\text{wt}\%)) \times 100 \\ \text{wt}\%$$

The SnSe<sub>2</sub> loadings in the SnSe<sub>2</sub>@NC and SnSe<sub>2</sub>-SnO<sub>2</sub>@NC are calculated to be 34.5 and 63.4 wt%, corresponding to 65.5 and 36.6 wt% for N-C, respectively.

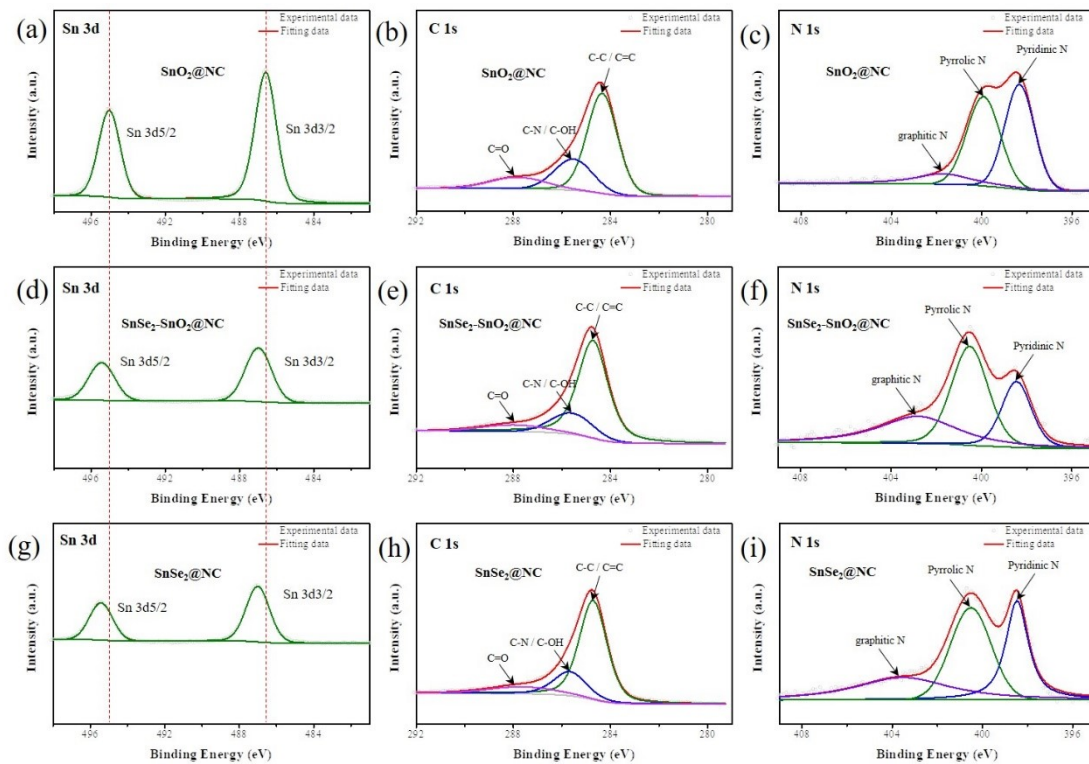
When Only the material of SnO<sub>2</sub> in the material, the SnO<sub>2</sub> content is estimated by

$$m(\text{SnO}_2) = m_2(\text{wt}\%) / m_1(\text{wt}\%) \times 100 \text{ wt}\%$$

The SnO<sub>2</sub> loadings in the SnO<sub>2</sub>@NC and SnSe<sub>2</sub>-SnO<sub>2</sub>@NC are calculated to be 58.3 and 34.5 wt%, corresponding to 31.7 and 35.5 wt% for N-C, respectively.

To sum up, the carbon content of SnSe<sub>2</sub>-SnO<sub>2</sub>@NC is between 35.5 wt% and 36.6 wt%. The carbon contents of SnO<sub>2</sub>@NC, SnSe<sub>2</sub>@NC is 31.7 and 65.5 wt%, respectively.

**Fig. S2.** High-resolution XPS spectra of (a), (d), (g) Sn 3d; (b), (e), (h) C 1s; and (c), (f), (i) N 1s for SnO<sub>2</sub>@NC, SnSe<sub>2</sub>@NC, and SnSe<sub>2</sub>-SnO<sub>2</sub>@NC microbelts, respectively.



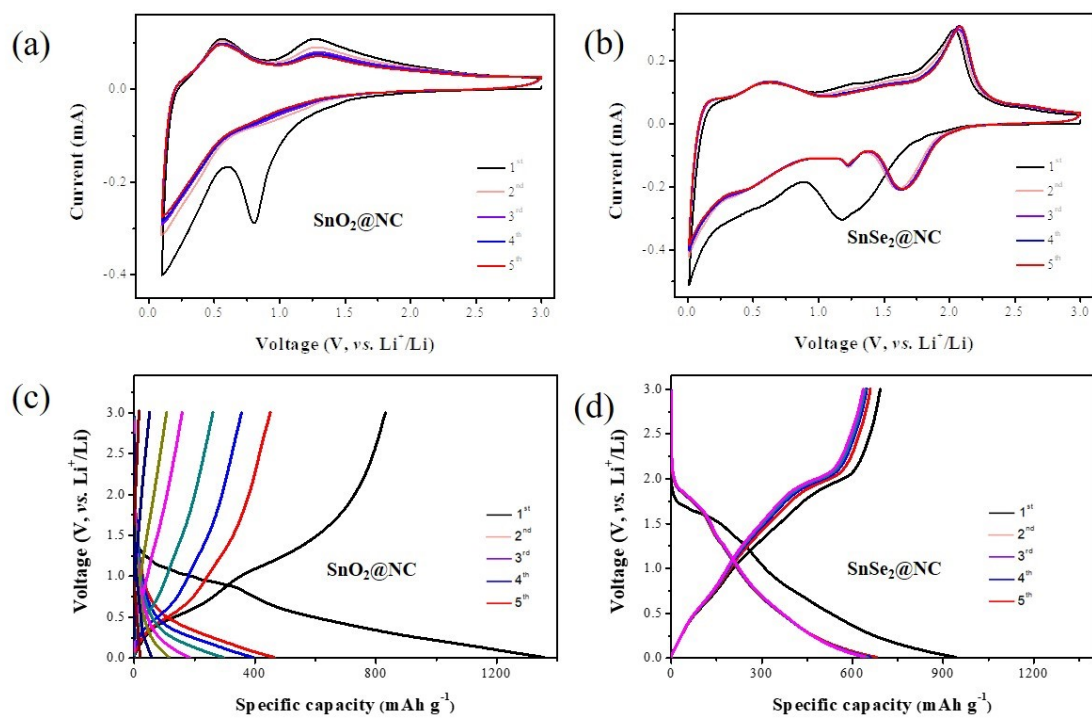


**Fig. S3.** (a,b) CV curves for the first five cycles of the SnO<sub>2</sub>@NC and SnSe<sub>2</sub>@NC electrodes at a scan rate of 0.2 mV s<sup>-1</sup>. (c,d) Galvanostatic discharge-charge curves for selected cycles of the SnO<sub>2</sub>@NC and SnSe<sub>2</sub>@NC electrodes at a current density of 0.2 A g<sup>-1</sup>.

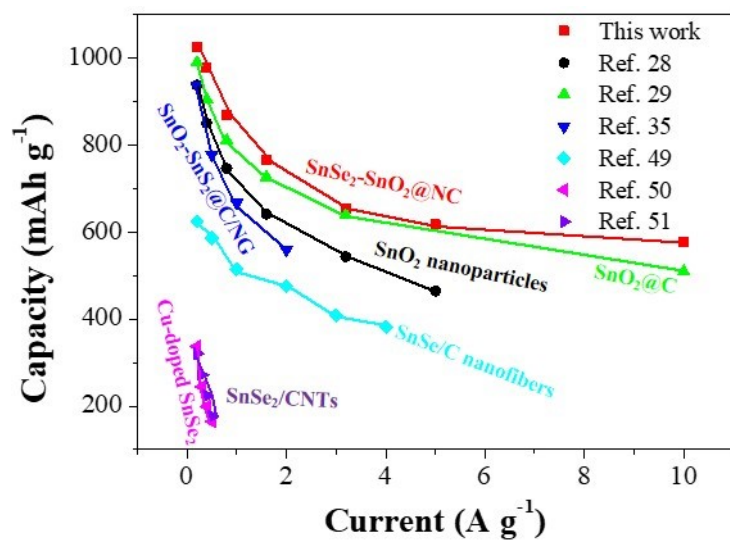


**Fig. S4.** Comparisons of the rate performance of the SnSe<sub>2</sub>-SnO<sub>2</sub>@NC with those of other similar reported anode materials.

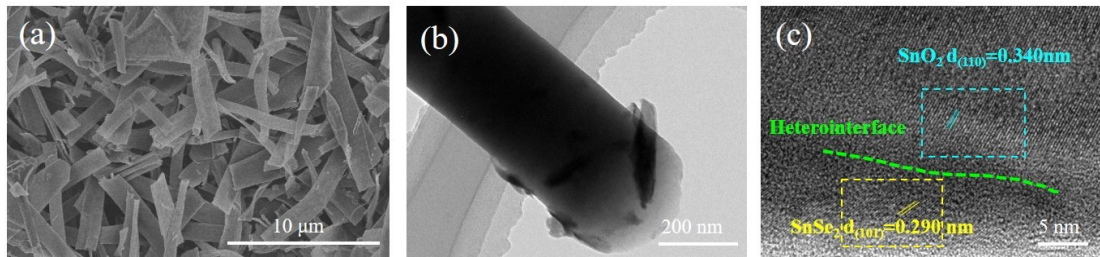


**Fig. S5.** SEM and High-resolution TEM images of the cycled  $\text{SnSe}_2\text{-SnO}_2\text{@NC}$  electrode.



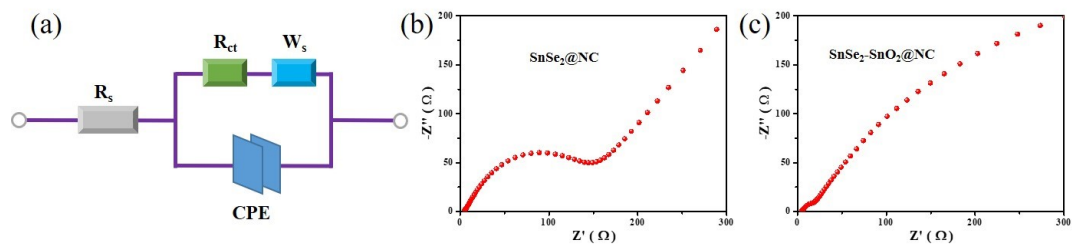


**Fig. S6.** (a) An equivalent circuit model for fitting of the Nyquist plots of the electrodes. (b,c) Nyquist plots of  $\text{SnSe}_2@NC$  and  $\text{SnSe}_2\text{-SnO}_2@NC$  electrodes.

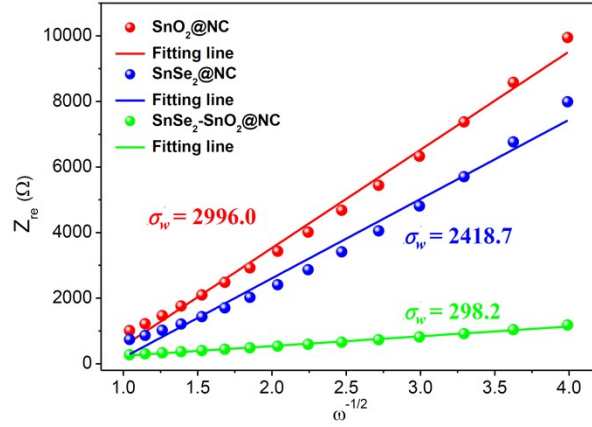


**Fig. S7.**  $Z' - \omega^{-0.5}$  plots in the low frequency range for  $\text{SnSe}_2@\text{NC}$  and  $\text{SnSe}_2\text{-SnO}_2@\text{NC}$  electrodes

To further investigate the electrode kinetics, the  $\text{Li}^+$  diffusion coefficient ( $D_{\text{Li}^+}$ ) is also calculated through the linear fitting of  $Z_{\text{re}}$  vs.  $\omega^{-1/2}$  (Fig. S7). The detailed calculation is based on the following equation formulas:

$$Z' = R_s + R_{ct} + \sigma \omega^{-1/2} \quad (\text{S5})$$

$$D_{\text{Li}^+} = \frac{R^2 T^2}{2 A^2 n^4 F^4 C^2 \sigma^2} \quad (\text{S6})$$

Where  $R$ ,  $T$ ,  $A$ ,  $F$ ,  $n$  and  $C$  are the gas constant ( $8.314 \text{ J K}^{-1} \text{ mol}^{-1}$ ), absolute temperature (298 K), the area of electrode surface, Faraday constant ( $96500 \text{ C mol}^{-1}$ ), number of transferred electrons and concentration of the  $\text{Li}^+$  ( $\text{mol cm}^{-3}$ ), respectively. As a result, the  $\text{SnSe}_2\text{-SnO}_2@\text{NC}$  has a smaller  $\sigma$  value of 298.2 than  $\text{SnSe}_2@\text{NC}$  (2418.7) and  $\text{SnO}_2@\text{NC}$  (2996.0), once again indicating its stronger diffusion dynamics of  $\text{Li}^+$ .